THE 27-28 OCTOBER 1986 FIRE IFO CIRRUS CASE STUDY: COMPARISON OF SATELLITE AND AIRCRAFT DERIVED PARTICLE SIZE

Bruce A. Wielicki and J. T. Suttles
Atmospheric Sciences Division, NASA Langley Research Center
Hampton, Virginia

Andrew J. Heymsfield
National Center for Atmospheric Research, Boulder, Colorado

Ronald M. Welch
South Dakota School of Mines and Technology, Rapid City, South Dakota

James D. Spinhirne and Man-Li C. Wu
NASA Goddard Space Flight Center, Greenbelt, Maryland

David O'C. Starr
NASA Goddard Space Flight Center, Greenbelt, Maryland

Lindsay Parker and Robert F. Arduini
PRC Corporation, Hampton, Virginia

1. INTRODUCTION

Theoretical calculations predict that cloud reflectance in near-infrared windows such as those at 1.6μm and 2.2μm should give lower reflectances than at visible wavelengths (Pollack et al., 1978; Hansen and Pollack,1970; Twomey, 1971). The reason for this difference is that ice and liquid water show significant absorption at these wavelengths, in contrast to the nearly conservative scattering at wavelengths shorter than 1μm. In addition, because the amount of absorption scales with the path length of radiation through the particle, increasing cloud particle size should lead to decreasing reflectances at 1.6μm and 2.2μm. Measurements at these wavelengths to date, however, have often given unpredicted results. Twomey and Cocks (1982) found unexpectedly high absorption (factors of 3 to 5) in optically thick liquid water clouds. Curran and Wu (1982) found unexpectedly low absorption in optically thick high clouds, and postulated the existence of supercooled small water droplets in place of the expected large ice particles. We will examine the implications of the FIRE data for optically thin cirrus.

2. RESULTS

The Landsat satellite has spectral bands at 0.83μm, 1.65μm, and 2.21μm which cover this range of variation in cloud absorption. Each pixel has a nominal spatial resolution of 28.5 meters. Figure 1 gives the region covered by the Landsat data over Lake Michigan on October 28, 1986. Figure 2 gives the Landsat measured nadir reflectance ratio R(2.21μm)/R(0.83μm) for the 58.4 km square analysis region (solid line) in Fig. 1. At 15:38:30 UTC the King Air aircraft took a direct sample of the cloud particles on an oil covered slide. The sample is shown in Fig. 3b and is dominated by water droplets with a mean radius of about 4μm. This sample corresponds to a reflectance ratio of about 0.75 found in the Landsat data at location "1" in Fig. 2. There is a time difference of 15 minutes between the King Air and Landsat observations. The liquid water regions of this cloud, however, appear to have been colloidally stable (Heymsfield et al, 1989). A second direct cloud particle sample was collected at 15:52 UTC. This sample is shown in Fig. 3a and contains only ice particles (broken spatial plates and some columns, 20 to 300μm in length). This second sample corresponds to a reflectance ratio of about 0.4 found in the Landsat data at location "2" in Fig. 2. Note that the reflectances used to derive the image in Fig. 2 are not corrected for surface reflectance. In this case the reflectance ratios are a mixture of clear and cloudy signatures.

Given this qualitative agreement between the satellite and aircraft data, the next step is to test the quantitative agreement along the King Air aircraft track. The Landsat radiance data are spatially averaged to 1 km resolution, sampled every 0.5 km along the King Air groundtrack. Cloud reflectances are then corrected for surface reflectance effects as in Platt et al (1980). The 1.65μm and 2.21μm channels are found to require less than 0.01 correction for surface reflectance. The correction for the 0.83μm channel is less than 0.05.

Figure 4 compares theoretical radiance calculations using the Finite Difference method (Suttles, 1981, 1985; Barkstrom, 1976) with the measured nadir cloud reflectance at 0.83μm and at both 1.65μm and 2.21μm along the King Air groundtrack. Calculations use a solar zenith angle of 60^0. The phase function for ice particles is taken from the laboratory measurements of Volkovitskiy et al (1980). The phase function for water particles is taken from theoretical Mie calculations with an effective radius of 3.8μm. Figures 4a and b give results for 1.65μm. Figures 4c and 4d give results for 2.21μm. The Landsat data are shown with symbols indicating the corresponding portion of the King Air track shown in Fig. 2.

It is evident that there are two distinct populations of cloud particles along the 88 km track. The high reflectance ratio values in Fig. 2 (15:38:10-15:39:09 UTC and 15:49:40-15:50:39 UTC) appear along the diagonal of nearly equal reflectance at the two wavelengths and are consistent with water droplets or ice spheres with radius less than 7.5μm. The remaining data indicate larger particles of about 60μm radius. Examination of the 1.65μm versus 2.21μm data given in Fig. 4 indicates that the large particles are ice. An assumption of liquid water for the large particles would give inconsistent particle sizes at 1.65 and 2.21μm. An assumption of ice gives consistent particle size in the two wavelengths. The small particles are too small to reliably distinguish ice from liquid water phase for these optically thin clouds.

Figure 5 gives the King Air particle size distributions using the combined FSSP, 2D-C, and 2D-P probes. For the 2D-C and 2D-P probes, particle size is calculated as a sphere with cross-section area πr^2 equal to the area of the particle image in the 2-D probe. For compact non-spherical particles, this specification is similar to using equivalent volume spheres (Pollack and Cuzzi, 1980). Pollack and Cuzzi (1980) found that for large size parameter $x = 2\pi r/\lambda >> 1$, and moderate absorption $2n'x < 1$) (where n' is the imaginary index of refraction), equivalent volume spheres are most accurate for absorption efficiency determination. For the 1.65μm and 2.21μm spectral bands, the appropriate radius range would be from about 3μm to 400μm. Given the compact particle habits observed in the microphysical data, the use of equivalent cross-section area spheres should be reasonably accurate. Large aspect ratio particles would lead to an overestimate of the true particle volume, and therefore an overestimate in particle absorption at 1.65 and 2.21μm. Such particles, however, were rarely noted in the data.

Four characteristic size distributions are given in Fig. 5. The data for 15:38:10 to 15:39:09 UTC cover the high ratio of R(2.21)/R(0.83) found in Fig. 2 near the location "1" in the figure. The microphysical data are dominated by small water droplets with radius about 4μm. The next section of the flight track (15:39:10 to 15:45:24 UTC) shows a peak at about 150μm, but no water droplets. The third section (15:49:40 to 15:50:39 UTC) has the smallest particle concentrations, and is taken from the high ratio of R(2.21)/R(0.83) found just before the end of the King Air track in the Landsat image. The Landsat data imply small particle sizes, while the aircraft finds no small drops in the FSSP probe. Spinhirne and Hart (1989) noted from the ER-2 lidar data (ground track shown in Fig. 2) that the mixed phase cloud occurred in vertically thin layers (100 - 200 meters thick) at heights between 7.3 and 8.0 km. The lidar depolarization data at location '1' in Fig. 2 verifies the existence of a mixed ice/liquid water phase cloud layer at 7.3 km altitude (Spinhirne and Hart, 1989), the position of the King Air at 15:38:30 UTC. The King Air altitude at 15:50 UTC is 7.0 km, which is below the lidar detected altitudes for mixed phase cloud. It is likely that the King Air data at 15:50 missed the liquid water layer. We conclude that the aircraft microphysics and Landsat reflectances are in qualitative agreement, subject to uncertainties in the vertical variation of cloud microphysics and temporal evolution of the cloud field.

The quantitative comparison of aircraft and radiometrically derived particle size requires the determination of an effective mean particle radius. Figure 6 gives the Landsat 2.21/0.83μm cloud reflectance ratio versus effective radius r_e. We define $r_e = \int r^3 N(r)dr \; / \; \int r^2 N(r)dr$, where

N(r) is the size distribution derived using the King Air microphysics data. This effective radius is a cross-section area weighted radius and has been shown useful in characterizing overall radiative properties of a particle size distribution. The number densities are averages over 5-second intervals, which results in size distributions representative of 500-meter sections of the cloud field.

Figure 6 indicates a significant but poor correlation between aircraft particle size and the 2.21/0.83μm reflectance ratio. There appear to be three clusters of data, one with r_e of about 4μm, and two with r_e about 200μm. The apparently anomalous data with large particle size and large reflectance ratio (15:50 UTC) are the liquid water layer missed by the King Air as discussed above. Recall that the data in Fig. 4 also clustered in two particle size groups, water droplets with radius less than 7.5 micron, and ice particles with radius about 60μm. While the water droplets appear consistent between the two data sources, the ice particles are in substantial disagreement, the radiative measurements indicating a smaller particle size by about a factor of 3. In order to understand this discrepancy, the uncertainties inherent in such a comparison are examined below.

i. Uncertain Index of Refraction: factor of 2.

Warren (1984) estimates that the uncertainty of the imaginary index of refraction for ice in the 1.4 to 2.8μm spectral region is a factor of 2.

ii. Uncertainty in the scattering phase function: ≈ 30%.

Use of the Mie scattering phase function in place of the VPP gave particle sizes about 60% smaller than those predicted in Fig. 4. This is an extreme test of the phase function.

iii. Uncertainty in the use of a single particle radius to represent an entire size distribution: ≈ 15% at r_e < 200μm.

Mie calculations were run to determine single scatter albedo as a function of r_e for the King Air size distributions (5 second averages) for each wavelength. These complete calculations were then compared to Mie calculations using a single particle size (as in Fig. 4).

iv. Uncertainty in converting 2D image area to equivalent sphere: Unknown.

The good agreement between the King Air median mass-weighted diameter determined as a function of crystal habit and 2 r_e determined using particle cross-section area (Fig. 6) argues that this error is of secondary importance.

v. Inadequate microphysical sampling: Unknown.

The size comparisons in Fig. 6 are given using the King Air measurements in the lower cloud layer at 7.3 km. Measurements of the upper cloud layer by the Sabreliner show mean particle radius decreasing from 200μm at 9 km to 40μm at 11 km. Note that a 20μm radius is the smallest particle size measured by the 2D-C probe at the Sabreliner airspeed. Many small particles in the upper cloud layer are undoubtedly missed by the 2D-C and 2D-P probes (Heymsfield et al, 1989). In support of this concern, Spinhirne and Hart (1989) estimate a mode radius of 20μm for the upper cirrus layer on October 28 using integrated lidar backscatter and 11μm emittance. For the lower cloud layer at 7-8 km, Fig. 5 shows that all of the 2-D size distributions at 7.3 km have maximum number density for the smallest particle size measured by the 2D-C probes. While the effect of these unsampled small ice particles on the determination of r_e is unknown, it seems reasonable from the size distributions shown in Fig. 5, that this effect alone might explain the discrepancy between 60 and 200μm values for r_e.

3. CONCLUSIONS

The FIRE October 28, 1986, data provide a unique opportunity to compare measured and theoretical cloud properties for cirrus clouds. Overall impressions are:

1. The lower cloud layer (7-8 km) appeared to dominate the cloud radiative properties as viewed by the ER-2 and Landsat. This result is consistent with the King Air and Sabreliner microphysical measurements and with ER-2 lidar observations.

2. Particle size inferred using Landsat cloud reflectance at 0.83μm, 1.65μm and 2.21μm gave good agreement with the King Air cloud particle samples for portions of the cloud field dominated by small water droplets with r_e = 3.8μm. For the larger ice crystals, the radiation measurements determined an r_e of about 60μm, compared to about 200μm determined using the King Air FSSP, 2D-C, and 2D-P probes. We conclude that the discrepancy is caused by two uncertainties. First, ice

particle sizes below about 20μm are not detected by the aircraft probes. The particle number densities are maximum at the smallest particles sensed by the 2-D probes, indicating the presence of smaller ice particles, even in the radiatively dominant lower cloud layer at 7-8 km. Second, uncertainties in the imaginary index of ice for the 1.65 and 2.21μm spectral bands causes an uncertainty of a factor of two in the Landsat derived particle size. The effect of small ice particles in the upper cirrus layer at 9-11.6 km is estimated to be of secondary importance.

3. Recommendations for future cirrus experiments include improved measurement of ice particle concentrations for sizes between 1 and 50μm, improved sampling of the vertical variation of cloud microphysics, more accurate radiometric calibration of aircraft radiometers, and more accurate values for the imaginary index of ice between 1.5 and 2.5μm wavelengths.

4. REFERENCES

Barkstrom, B. R., 1976: *J. Quant. Spect. Rad. Transf.*, **16**, 725-739.

Curran, R. J. and M.-L. C. Wu, 1982: *Jour. Atm. Sci.*, **39**, 635-647.

Foot, J. S., 1988: *Q. J. R. Meteor. Soc.*, **114**, 145-164.

Hansen, J. E., and J. B. Pollack, 1970: *J. Atmos. Sci.*, **27**, 265-281.

Heymsfield, A. J., and C. M. R. Platt, 1984: *J. Atmos. Sci.*, **41**, 846-855.

Heymsfield, A. J., K. M. Miller, and J. D. Spinhirne, 1989: Submitted to *Mon. Wea. Rev.*

Markham, B. L., and J. L. Barker, 1986: *EOSAT Landsat Technical Notes*, No. 1, August, 1986.

Platt, C. M. R., D. W. Reynolds, and N. L. Abshire, 1980: *Mon. Wea. Rev.*, **108**, 195-204.

Pollack, J. B., and J. N. Cuzzi, 1980: *J. Atmos. Sci.*, **37**, 868-881.

Spinhirne, J. D., and W. D. Hart, 1989: Submitted to *Mon. Wea. Rev.*

Suttles, J. T., 1981: Ph.D. Thesis, Old Dominion University, Norfolk, VA., 180 pp.

Suttles, J. T., 1985: In Radiative Transfer in Scattering and Absorbing Atmospheres. Edited by J. Lenoble, A. Deepak Publishing.

Takano, Y., and K-N Liou, 1989: *J. Atmos. Sci*, **46**, 3-19.

Twomey, S., 1971: *J. Quant. Spectros. Radiat. Transfer*, **11**, 779-783.

Twomey, S. and T. Cocks, 1982: *J. Met. Soc. Japan*, **60**, 583-592.

Volkovitskiy, et al., 1980: *Izvestiya, Atm. and Ocean. Phys.*, **16**, 98-102.

Warren, S. G., 1984: *Appl. Opt.*, **23**, 1206-1225.

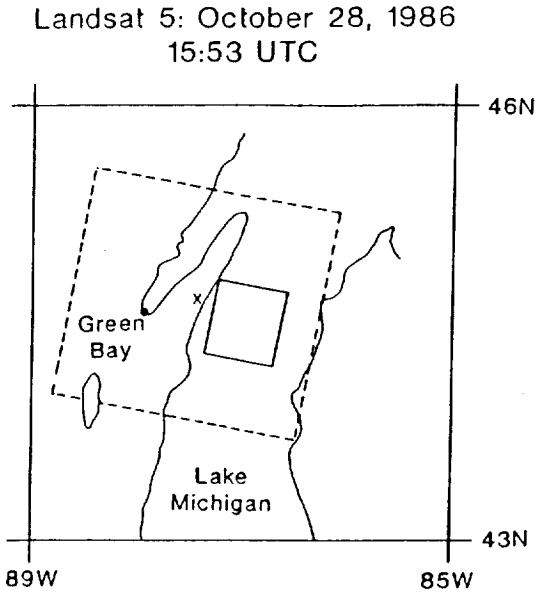

Fig. 1. Location of the Landsat image area for the study. Solid line box gives the 58.4 km square area over Lake Michigan analyzed and shown in Fig. 2.

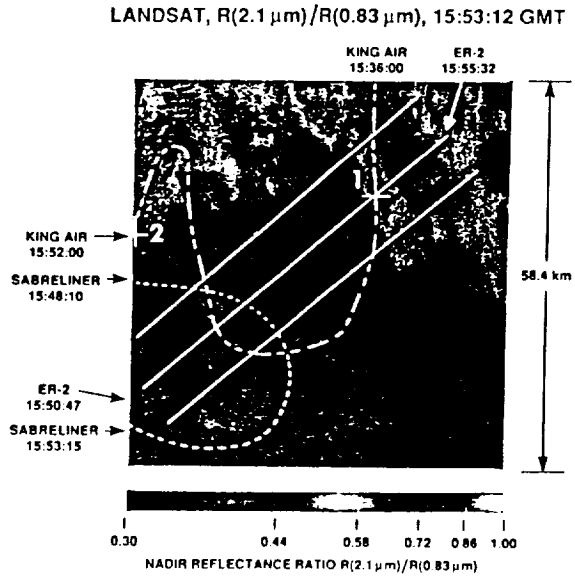

Fig. 2. Landsat reflectance ratio, R(2.21μm)/R(0.83μm) over the analysis area. Aircraft tracks and observation times are also given in the figure. Data in Figs. 5 and 6 is taken along the King Air ground track.

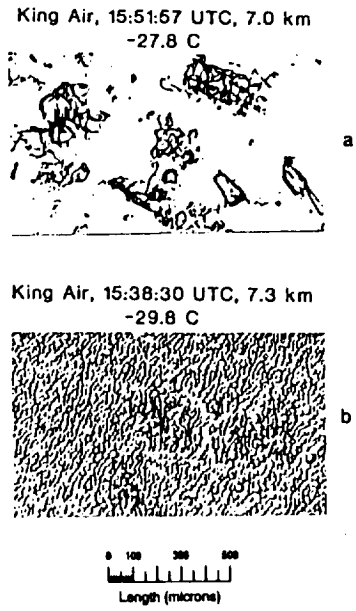

Fig. 3. Photographs of cirrus particles collected by the King Air on oil coated slides. 3a shows ice crystals collected at 15:51:57 UTC and corresponds to location "2" in Fig. 2. 3b shows water droplets collected at 15:38:30 UTC, and corresponds to location "1" in Fig. 2.

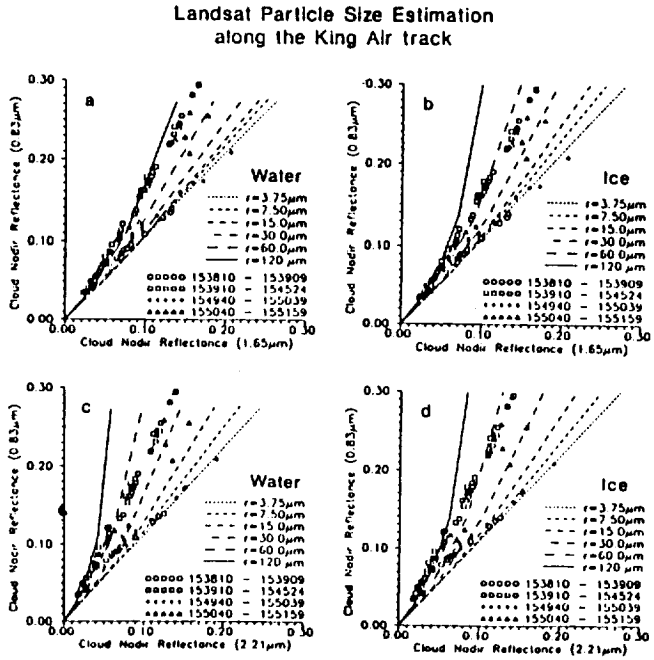

Fig. 4. Measured and calculated cloud nadir reflectance. Landsat observations are taken along the King Air ground track seen in Fig. 2. Theoretical calculations use the VPP ice scattering phase function and Mie single scatter albedos as a function of particle radius. 4a and 4b give results for R(0.83μm) vs. R(1.65μm) for liquid water (a) and ice (b) refractive index. 4c and 4d give results for R(0.83μm) vs. R(2.21μm) for liquid water (c) and ice (d) refractive index.

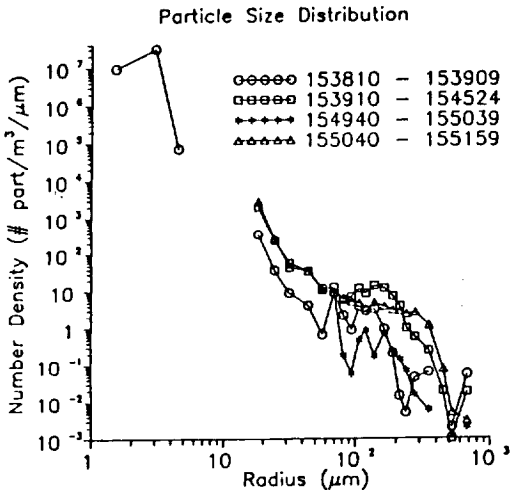

Fig. 5. King Air measured cirrus size distributions using the FSSP, 2D-C and 2D-P probes. Particle size for 2D probes is that of a sphere with equivalent cross-section area to the particle 2-D image. Size distributions are averaged over the time intervals shown in the figure.

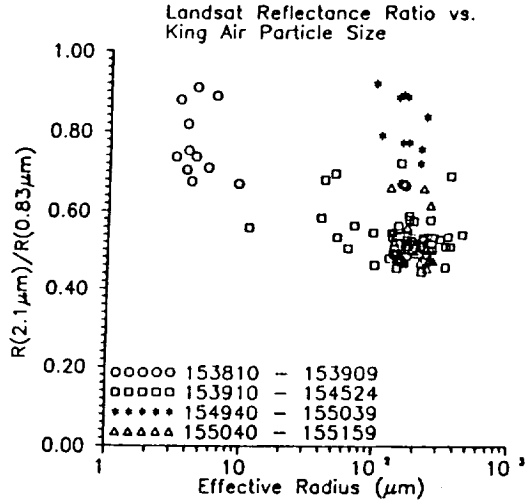

Fig. 6. Comparison of Landsat measured cloud reflectance ratio R(2.21μm)/R(0.83μm) with the King Air determined effective radius r_e.